

Development of a Verified Distal End for 3D-Printed Transtibial Prosthetic Sockets

A Thesis  
SUBMITTED TO THE FACULTY OF THE  
UNIVERSITY OF MINNESOTA  
BY

Ian Douglas Knoll

IN PARTIAL FULFILLMENT OF THE REQUIREMENTS  
FOR THE DEGREE OF  
MASTER OF SCIENCE

Dr. Andrew Hansen

December 2023

Ian Douglas Knoll 2023 ©

## **Acknowledgements**

I would like to thank my advisor Dr. Andrew Hansen for his support and guidance over the last three years, in matters both academic and professional. Thank you for helping me engage in research that has been equal parts challenging and rewarding. On a similar note, I would like to thank Eric Nickel for serving as an unofficial advisor, providing me with the knowledge and resources I needed to succeed, and putting up with a near constant stream of modeling troubleshooting. I would further like to thank all the members of my thesis committee for the time they have volunteered and for helping me make this document the best it could be.

On a logistical level, I want to thank Alexander Berardo-Cates for his insight and for organizing the printing of the prosthetic sockets used in this research, as well as the mechanical testing of the tensile bars referenced within. I would also like to thank the Minneapolis VA Medical Center for allowing me to use their space and resources, with particular thanks going to the RECOVER center for the use of their socket testing system.

Finally, I would like to thank anyone and everyone who has offered me support throughout my academic career, be it a kind word or a keen mind to bounce ideas off of. This work is a direct result of your encouragement and would not have been possible otherwise.

## **Abstract**

*Background:* An ideal lower limb prosthetic socket should be comfortable and durable while minimizing weight; optimizing socket designs for these goals can prove difficult due to the bespoke nature of definitive sockets. ISO 10328 is designed to verify the strength and durability of engineered prosthetic components but is commonly adapted for socket research. Sockets tested with ISO 10328 loading conditions typically fail at the distal end. Traditional socket fabrication methods involve downsides including long lead times, substantial labor, and variable quality brought on by manual fabrication. 3D-printing has been proposed as an alternative, but 3D-printed socket designs, most notably the distal end, are typically based on laminated sockets rather than taking advantage of the medium's ability to generate complex geometry.

*Objectives:* To design transtibial socket distal end geometry that can be used in 3D printed sockets across a variety of limb sizes and shapes, and to provide verification data from modified ISO 10328 testing that presents criteria for the merging radius between the socket body and distal end as well as evidence of the resulting load capacity.

*Methods:* Using Topology Optimization, a distal end was modeled from simulated ISO 10328 conditions representing loads expected of a 125 kg user. Socket assemblies were designed using the distal end and tested with FEA to assess socket design criteria based on distal end build height and merging radius. Three example sockets were printed and tested under ISO 10328 ultimate strength criteria to the P6 level in Condition II for comparison to FEA results.

*Results:* FEA testing suggested a minimum merging radius of 6 cm would produce a socket capable of withstanding P6 load levels. Build height should be minimized as much

as possible without interfering with the merging radius. Experimental testing supports these conclusions, with sockets designed within these criteria withstanding the P6 ultimate strength maximum, and a socket violating the criteria failing at a lower load. All sockets failed in locations consistent with FEA modeling.

*Conclusions:* Using Topology Optimization and FEA, 3D-printed prosthetic sockets that are both lightweight and durable were designed. The techniques and results presented offer a framework by which a distal end viable over a range of socket designs could be produced.

## Table of Contents

Acknowledgments.....	i
Abstract.....	ii
List of Tables .....	v
List of Figures.....	vi
List of Abbreviations .....	viii
Introduction.....	1
Methods.....	4
<i>Topology Optimization</i> .....	4
<i>FEA Testing</i> .....	6
<i>Socket Manufacturing</i> .....	8
<i>Socket Testing</i> .....	9
Results.....	11
<i>FEA Results</i> .....	11
<i>Experimental Results</i> .....	12
Discussion .....	16
Conclusions.....	19
Bibliography .....	20

## List of Tables

Results.....	11
<i>Table 1. Tensile bar elastic modulus and tensile stress at max force for printed sockets. ....</i>	<i>13</i>
<i>Table 2. Design settings, maximum load, and failure mode for printed sockets. ..</i>	<i>13</i>

## List of Figures

Methods.....	4
<i>Figure 1. Topology optimization setup, design space darkened for emphasis. ....</i>	<i>5</i>
<i>Figure 2. Topology optimization results (i) initial output, sagittal view; (ii) initial output, angled view; (iii) refined model, sagittal view; (iv) refined model, angled view. ....</i>	<i>6</i>
<i>Figure 3. Connection of distal module to socket body (i) before edge smoothing; (ii) after smoothing, transitional face outlined in white. ....</i>	<i>7</i>
<i>Figure 4. Example contiguous iso-clipping results, full model transparent for comparison, focus areas circled for emphasis (i) transitional face results; (ii) posterior-medial slot results. ....</i>	<i>8</i>
<i>Figure 5. Example print layout, including Socket A and ISO 527 type 1A tensile bars. Socket offset from printer bed by 30mm to aid material consistency. ....</i>	<i>9</i>
<i>Figure 6. Experimental setup for ISO 10328 P6 Condition II ultimate strength test (Socket A). ....</i>	<i>10</i>
Results.....	11
<i>Figure 7. FEA results for varying build height. Merging radius held constant at 2 cm. Stress values are maximums based on iso-clipping. ....</i>	<i>11</i>
<i>Figure 8. FEA results for varying merging radius. Build height held constant at 5.414 cm. Stress values are maximums based on iso-clipping. Asterix indicates a value below the yield stress. ....</i>	<i>12</i>
<i>Figure 9. Failure mode for Socket A (i) distal module struts; (ii) socket body. ....</i>	<i>14</i>
<i>Figure 10. Failure mode for Socket C. ....</i>	<i>14</i>

*Figure 11. Example material deformation taken from Socket A (i) depression in anterior strut from pyramid adapter; (ii) depression in posterior strut from hex nuts.....15*

## List of Abbreviations

ISO .....	International Standards Organization
3DP .....	3D Printing
CAD .....	Computer Aided Design
FEA .....	Finite Element Analysis
TO .....	Topology Optimization

## **Introduction**

As the interface between residual limb and prosthesis, the prosthetic socket plays a vital role in the functionality and adoption of prosthetic limbs. An ideal lower limb prosthetic socket offers comfort and durability while minimizing the overall weight and physical profile.<sup>1</sup> While the end user benefits from a well optimized design, difficulties arise due to the bespoke nature of sockets. Unlike most prosthetic components, sockets must be custom designed for each user, and thus lack widely recognized guidelines for manufacturing and testing.<sup>1</sup> For engineered prosthetic components, the International Standards Organization (ISO) 10328 test standard is used to verify strength and durability.<sup>2</sup> Though excluded from the standard, ISO 10328 is commonly adapted in research to assess socket strength.<sup>1</sup> Multiple studies have demonstrated professionally fabricated sockets failing ISO 10328 loading, indicating the potential for further improvements to socket durability.<sup>3-5</sup> Due to the use of a rigid mock limb concentrating forces at the distal end, sockets which fail ISO 10328 loading typically fail at the point of attachment to pyramid adaptors or within the cup region.<sup>4-10</sup> While adding excessive material can alleviate these issues, doing so leads to unnecessary weight, potentially decreasing comfort and leading to fatigue for the prosthesis user.

Traditionally, definitive lower limb sockets are fabricated via lamination with composite materials including carbon fiber, Nyglass, and resin.<sup>1,5</sup> Lamination is typically performed manually, leading to long lead times, substantial labor from technicians and prosthetists, and variable build quality.<sup>5,11</sup> In recent years, 3D Printing (3DP) has been proposed as an alternative. Although concern has been placed on the mechanical strength of 3DP materials, research by Pousett et al.<sup>3</sup> and Owen and DesJardins<sup>10</sup> has

demonstrated that properly designed 3DP sockets can withstand ISO 10328 loading and perform comparably to traditional sockets. Additionally, 3DP offers benefits including introducing complex geometry difficult to replicate by hand, remote fabrication, and the maintenance of a digital database of limb shapes and socket designs to aid in future design and research.<sup>12</sup> Despite these potential benefits, many prosthetists lack the knowledge or experience with 3DP to design and fabricate sockets that are structurally sound and take advantage of the strengths of 3DP.

Because 3D printed sockets are typically designed with Computer Aided Design (CAD) software, tools such as Finite Element Analysis (FEA) can be utilized to improve socket design. FEA is a computer aided method of structural analysis that can determine deformations and stress distributions across a body under prescribed loading and support conditions. Such analysis can aid in design by offering insight into high stress regions prone to failure and minimal stress regions unnecessary to overall strength and durability. Previously, Marinopoulos et al.<sup>13</sup> used FEA to simulate ISO 10328 loading conditions on a 3DP socket and generated a modified design with variable thickness based on the distributions of stress across its surface. When tested experimentally under ISO 10328 conditions, these sockets demonstrated improved or comparable performance to the original design.<sup>13</sup> Topology Optimization (TO) can further these principles by offering an algorithmic approach for removing material from a design space based on FEA results, generating geometry that can inspire design optimization. Lindberg et al.<sup>14</sup> used this approach to design an optimized model of a simplified socket distal end based on ISO 10328 loading. While experimental testing showed this model failed at lower loads than

the original, the researchers demonstrated that FEA offered reasonable estimates of the loading limit and location of failure for both models.<sup>14</sup>

The purpose of this study was to develop geometry for 3DP transtibial prostheses that could be used over a range of socket sizes and shapes. As it is prone to failure and the area least reliant on limb geometry, the goal was to develop an optimized distal end (hereafter “distal module”) that could be incorporated into the CAD model of any transtibial socket meeting pre-determined geometric criteria. By presenting a framework for designing verified socket geometry, we hope to inspire the generation of models that will streamline fabrication and increase user confidence in 3D-printed sockets.

## **Methods**

### *Topology Optimization*

To optimize the distal end, an initial model was generated using commercial CAD software Fusion 360™. The model was designed as a cylindrical body with holes and slots to permit M6 bolts and hex nuts for the attachment of a generic pyramid adaptor. The top of the model was connected to a 5 mm thick conical shape to simulate a generic socket shape. In addition, a loading platform was modeled to enable simulation of ISO 10328 loading conditions. The platform consists of a plate with indents on the distal face positioned to match load application offsets for ISO 10328 P6 Condition I (heel loading) and Condition II (forefoot loading). The offset positions are based on approximations of the position of the distal module when attached to a typical transtibial socket. The indents are angled to align the normal vectors with the loading vectors for P6 Condition I and II. Embossed into the proximal face of the loading platform is a surface matching the profile and thickness of a generic pyramid adaptor, from which geometry mimicking the bolt and hex nut assembly is attached.

Together, these models were imported and assembled in commercial topology optimization software Altair Inspire™ (Figure 1). The proximal face of the simplified socket was treated as fixed, while forces were applied via the loading platform. Contact between the two models was treated as sliding. All materials were assumed isotropic and linear elastic, with the loading platform treated as AISI 304 steel (elastic modulus 195 GPa) and the socket treated as Nylon 12 (elastic modulus 1.7 GPa). The distal module was assigned as the design space from which TO would remove material, excluding a 1 mm shell around regions vital to interfacing with the socket body or pyramid adaptor. A

symmetry constraint was applied in the sagittal plane to ensure the model would be applicable to left and right leg prostheses.

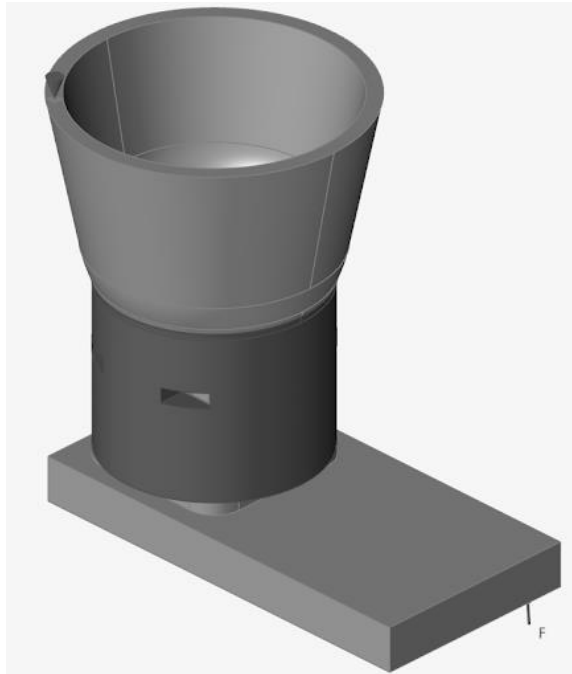


**Figure 1.** Topology optimization setup, design space darkened for emphasis.

Loading was applied in four separate conditions based on ISO 10328 P6 standards that would collectively influence optimization results: The Condition I and II P6 ultimate strength force minimums (3760 N and 3419 N respectively) applied at the corresponding indentations, and 50 N\*m applied as a positive or negative moment about the central axis of the embossed face. P6 loading is representative of users with a body mass of up to 125 kg (275 lbs). Based on preliminary testing, optimization was performed to maximize stiffness for a 50% mass reduction, as further reduction failed predetermined safety criteria. The resulting model was imported into Fusion 360™ to guide the generation of updated distal module geometry (Figure 2). At this time, the model was updated to include a 0.6mm clearance in the holes and slots, and to smooth any sharp edges in the slot interiors. An elevated vacuum suspension socket design was assumed.

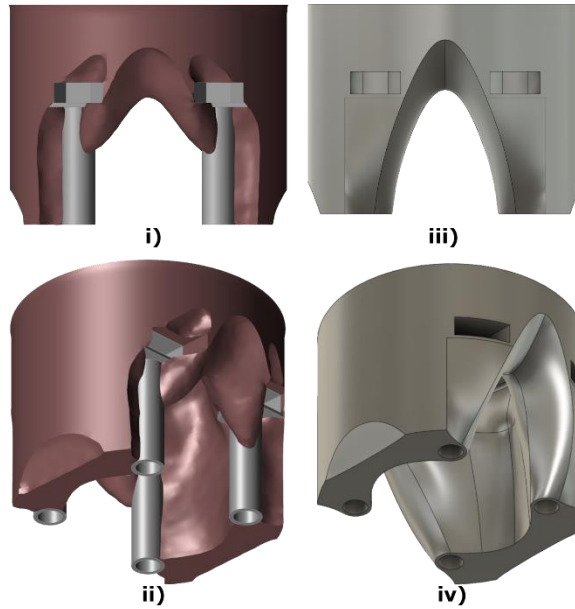


**Figure 2.** Topology optimization results (i) initial output, sagittal view; (ii) initial output, angled view; (iii) refined model, sagittal view; (iv) refined model, angled view.

### *FEA Testing*

To evaluate the impact of the updated distal module geometry on overall socket strength, FEA was performed. A 5 mm thick socket body was generated in Fusion 360™ based on a “typical” limb that had been scanned and modified to remove identifying details. The distal module was aligned approximately 1 mm below the internal face of the socket, then extended upwards and merged to form a single body. The edge between the socket and distal module was smoothed to a curved surface with a known radius, hereafter the “transitional face” and “merging radius” respectively (Figure 3). Socket assemblies were generated using a range of merging radii and build heights, the latter accomplished by scaling the distal module along the vertical axis. Corresponding loading platforms with adjusted bolt heights were also generated. In both cases, one variable was held fixed while the other was modulated.

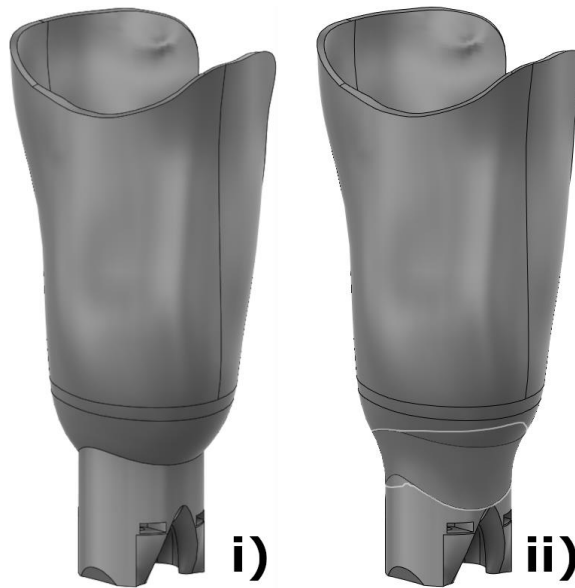


**Figure 3.** Connection of distal module to socket body (i) before edge smoothing; (ii) after smoothing, transitional face outlined in white.

FEA was performed in SolidWorks™ 2022 for each socket assembly. The interior of the socket was held fixed in the proximal region but kept free in the distal cap region, in accordance with ISO 10328 guidelines, which state that “The distal portion of the socket... shall either be a void or be filled with foam or soft materials, in order to allow this portion to deform freely under load.”<sup>2</sup> Contact was identical to the TO setup, save treating the hex nuts and their slots as bonded to account for the added clearance. Socket material properties were updated based on technical data for HP 3D High Reusability PA 12 (elastic modulus 1.8 GPa)<sup>15</sup> for consistency with experimental testing, while the loading platform remained unchanged. Loading was applied identical to the TO setup, with only Condition II tested. Compared to Condition I, this generates a greater moment at the distal end, constituting a worst-case loading condition. The load magnitude was set to the Condition II P6 ultimate static force maximum (4425 N) to better reflect the brittle failure mode of most 3D-printed sockets.

Results were analyzed using iso-clipping to factor out artifacts present in the stress distribution. Iso-clipping is a visual tool in SolidWorks™ 2022 that filters FEA results to only show mesh model nodes above a user-selected stress value. Using this tool, the filtered stress value can be lowered until a contiguous region of nodes is visible (Figure 4), as opposed to disparate and individual nodes likely to be outliers produced due to inaccuracies or limitations in the FEA simulation. In this case the goal was to lower the filtered stress value until a contiguous region of stress nodes were visible that spanned multiple mesh facets. If additional stray stress nodes existed that were close to the contiguous region, then the filtered stress value was further lowered to see if the two would form a greater contiguous region. While iso-clipping values can be subjective, presenting them is a means to filter out inaccuracies in the FEA simulation and present more realistic stress values.

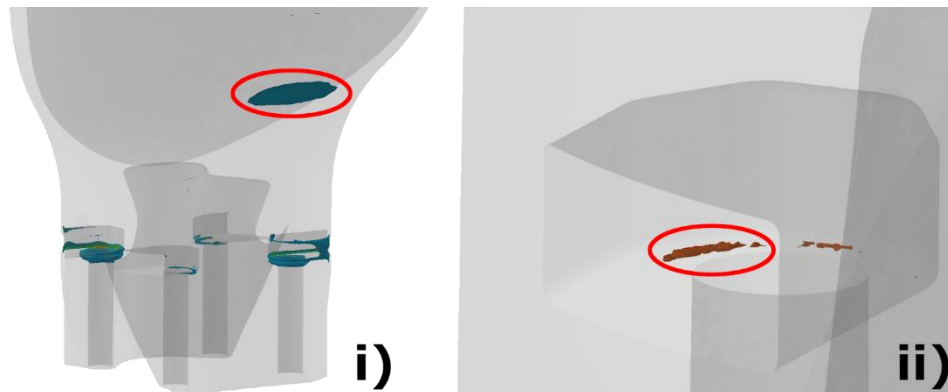


**Figure 4.** Example contiguous iso-clipping results, full model transparent for comparison, focus areas circled for emphasis (i) transitional face results; (ii) posterior-medial slot results.

### *Socket Manufacturing*

A set of three sockets (Sockets A, B, and C) were manufactured at the Richmond VA to compare with FEA testing. Socket designs were selected to represent the extremes

of the merging radii and build heights present in FEA. Before printing, socket models were converted to stl files with a 0.0275 mm and 0.5 degree tolerance and a maximum facet size of 3.335 mm. Sockets were printed on a HP Jet Fusion 580 Printer alongside a number of ISO 527 type 1A tensile bars (Figure 5). Tensile bars were tested in accordance with ISO 527-2 for the comparison of material properties with the values used in FEA.<sup>16</sup>

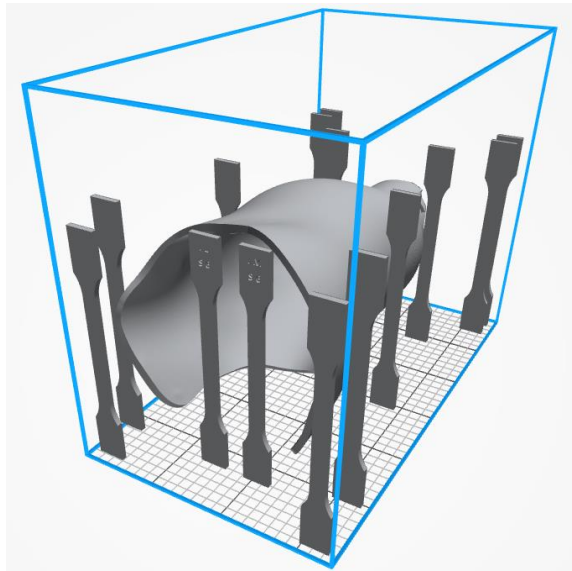


**Figure 5.** Example print layout, including Socket A and ISO 527 type 1A tensile bars. Socket offset from printer bed by 30mm to aid material consistency.

### *Socket Testing*

Experimental testing was performed at the Minneapolis VA Health Care System. Briefly, test specimens are placed between an actuator at the proximal end and an anchor point at the distal end, connected to both via a ball joint to allow for free rotation. Specimens consist of the socket, a limb dummy, and rigid elements simulating the pylon, foot, and pyramid adaptor (Figure 6). The rigid elements are positioned to establish load lines consistent with ISO 10328. The limb dummy is based on the same scan as the

sockets, with a prosthetic pylon surrounded by a hard resin limb. The limb shape is truncated approximately two inches from the distal end, consistent with ISO 10328 standards.



**Figure 6.** Experimental setup for ISO 10328 P6 Condition II ultimate strength test (Socket A).

During testing, six ply of prosthetic socks were placed on the limb dummy to adjust for a looser than anticipated fit. Further adjustments were made for Sockets B and C. The pyramid adapter height was increased by two spacer plates to properly fit the attachment bolts, and the distance between the loading and anchor points was increased by 18.9 mm. The latter was anticipated to increase the moment arm acting at the distal module by 0.429%, and was thus assumed to have a negligible impact on results.

Testing consisted of a 1100 N settling force, which is then ramped down to 200 N and held for ten seconds. Loading was then ramped until failure. To meet the ultimate

strength criteria for P6 Condition II loading, a specimen must maintain structural integrity without brittle failure until passing the upper threshold of 4425 N. Performance metrics for all specimens were compared to their corresponding FEA results.

## Results

### *FEA Results*

Figures 7 and 8 summarize FEA results as a function of build height and merging radius respectively. Results emphasize von Mises stress along the anterior transitional face and posterior-medial hex nut slot, as these areas experienced the highest stress concentrations. Dashed reference lines indicate the estimated yield strength based on technical data for HP 3D High Reusability PA 12.<sup>15</sup> Due to limitations in FEA and the mesh facet size used, stresses for the hex nut slot are not of accurate magnitude, and should be interpreted in terms of trends only. Stress along the transitional face had an inverse relationship with radius and build height, with radius having a more pronounced impact. Similar relationships are seen with slot stress, but the effect is not consistently linear; the impact of merging radius on slot stress is minor relative to build height.

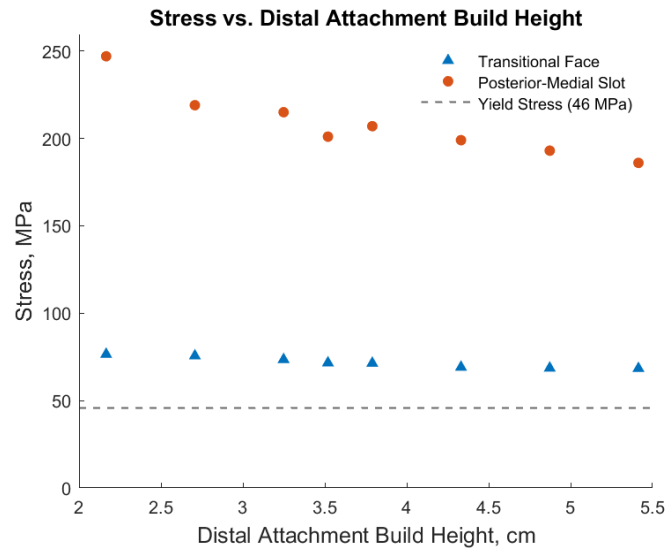


**Figure 7.** FEA results for varying build height. Merging radius held constant at 2 cm. Stress values are maximums based on iso-clipping.

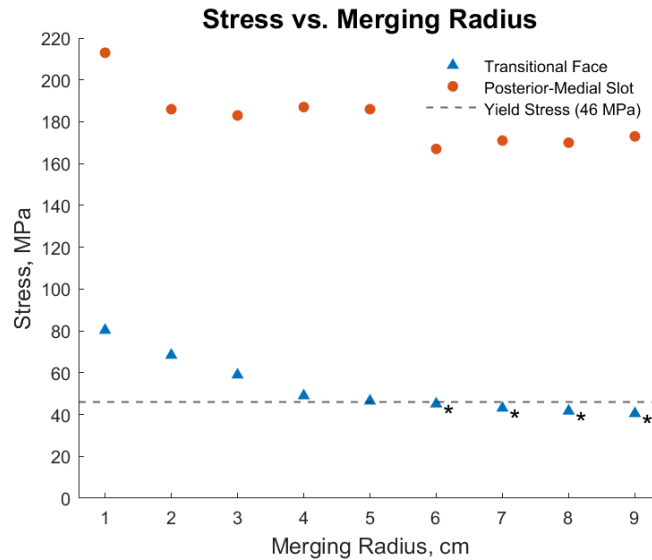


**Figure 8.** FEA results for varying merging radius. Build height held constant at 5.414 cm. Stress values are maximums based on iso-clipping. Asterix indicates a value below the yield stress.

### *Experimental Results*

Based on preliminary FEA results, three socket designs were chosen for experimental testing. Initial hypotheses suggested that radius of curvature would play a large role in ultimate strength. In comparison, it was hypothesized that the minimum build height required to accommodate a given merging radius being most optimal. As a result, a socket featuring the minimum merging radius below the yield strength in Figure 8 with the minimal build height required to accommodate said radius was chosen for testing (Socket A). For comparison, sockets featuring the same radius with maximum build height and a reduced merging radius with maximum build height were also manufactured (Socket B and Socket C). Material properties for the accompanying tensile bars are summarized in Table 1.

**Table 1.** Tensile bar elastic modulus and tensile stress at max force for printed sockets.

Socket	Elastic Modulus, GPa	Tensile Stress at Max Force, MPa
A	1.00985 (0.158271)	44.15 (0.973)
B	1.19602 (0.248562)	44.21 (3.756)
C	1.32321 (0.217817)	46.06 (0.774)

Ultimate strength values for each socket were taken as equivalent to the load at failure and are summarized alongside failure modes in Table 2. Sockets A and B satisfied the P6 Condition II upper threshold (4425 N), maxing out at 4502 N and 4480 N respectively. Socket C failed at a lower loading force (4357 N). Socket A failed along the hex nut slots, excluding the posterior-lateral slot (Figure 9). In addition, the posterior-lateral bolt sheared within the socket, preventing removal (Figure 9). Socket B exceeded the maximum actuator displacement before failure and was unable to be loaded further. Socket C failed at the transitional face, particularly along the anterior side (Figure 10). In all cases, deformation occurred at contact with the hex nuts and pyramid adaptor, with both elements recessing into the socket material. (Figure 11).

**Table 2.** Design settings, maximum load, and failure mode for printed sockets.

Socket	Merging Radius, cm	Build Height, cm	Maximum load, N	Failure Mode
A	6	3.520	4502	Failed along the hex nut slots: posterior strut broke off, both struts cracked at lateral side through hex nut slots
B	6	5.414	4480*	*N/A (Max displacement reached)
C	2	5.414	4357	Failed along transitional face: anterior side shattered into multiple pieces, while posterior side remained attached to distal module

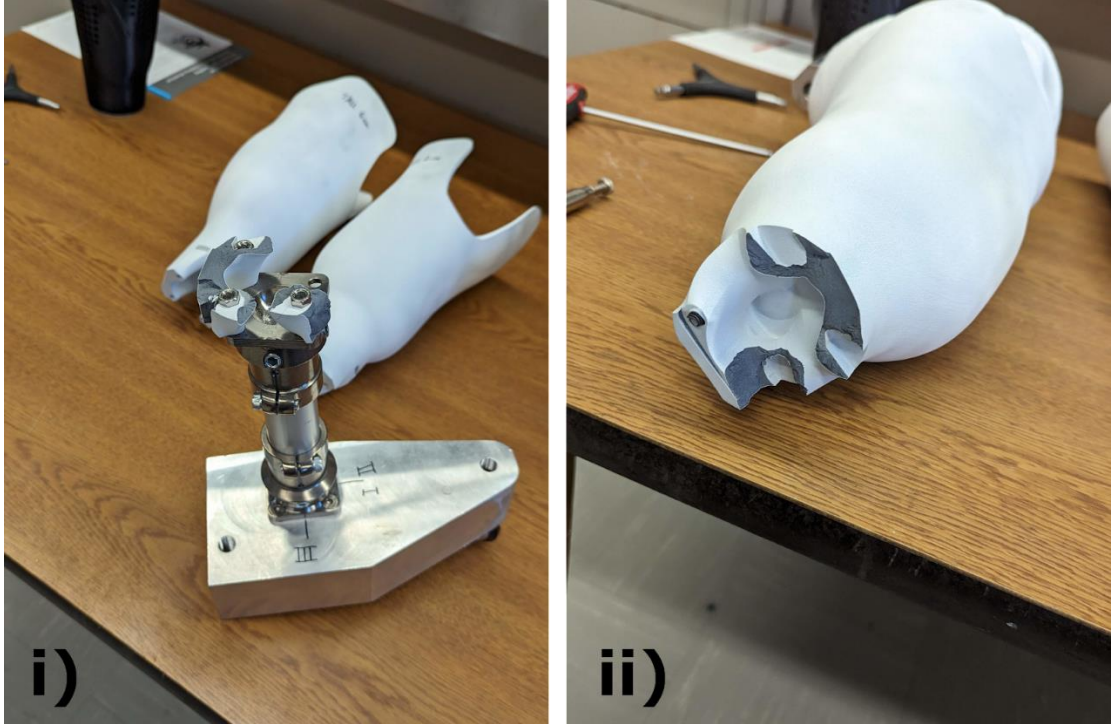


**Figure 9.** Failure mode for Socket A (i) distal module struts; (ii) socket body.



**Figure 10.** Failure mode for Socket C.

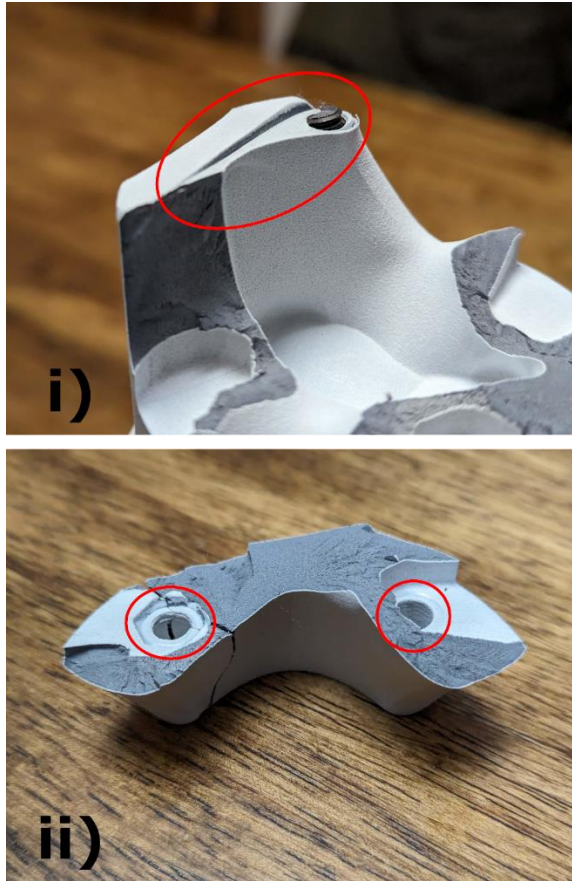


**Figure 11.** Example material deformation taken from Socket A (i) depression in anterior strut from pyramid adapter; (ii) depression in posterior strut from hex nuts.

## **Discussion**

The purpose of this study was to provide a preliminary framework for the design of a verified distal module. With the distal end being the region most prone to failure, a verified model would not only streamline fabrication, but offer prosthetists and users greater confidence in the strength of the final socket. Current results demonstrate the strength of this design iteration, as well as guidelines for its inclusion in definitive sockets. FEA testing suggests the merging radius should be at least 6 cm, with build height having minimal impact on strength along the transitional face. Experimental failure modes corroborate these guidelines. Socket A passing P6 loading criteria and failing along the posterior slots is consistent with these guidelines, as is Socket C failing below the loading criteria due to a reduced merging radius. While failure for Socket B was unable to be observed, maintaining a higher maximum load than Socket A is consistent with build height decreasing slot stress. While the inclusion of prosthetic socking does impact the accuracy of the experimental procedure, the cushioning would increase the moments experienced, and should not impact these conclusions. These results provide preliminary evidence of the distal module strength, the design criteria presented, and the value of using FEA to simulate ISO 10328 testing.

That said, FEA should be seen as an approximation of the scenarios modeled, and is best used to predict data trends and offer guidelines for experimental testing. The posterior-medial slot stresses in Figures 7 and 8 are a strong example of the limitations of FEA. Due to the slot geometry being of a small scale relative to the remaining socket, conventional mesh generation is likely to produce results too coarse to properly model the geometry, even if high resolution mesh settings are used. As a result, unrealistically

high stresses were observed in the region. As with any simulation, FEA is most powerful when a clear understanding of its limitations and inaccuracies is present.

While 3DP presents the opportunity to greatly improve socket design, doing so must be balanced with a reasonable concern for failure. 3DP materials are prone to brittle failure, presenting a risk of catastrophic failure occurring during active use, leading to injury and a decreased confidence in prosthesis usage. While failure in traditional sockets is rare, the ability to better optimize 3DP sockets has the potential to increase this risk. For 3DP to be viable, great care must be placed on the structural integrity of the resulting sockets. As Table 2 demonstrates, material properties can also vary greatly between prints, and may not conform directly to stated technical values. As with all manufacturing processes, a degree of safety factors must be put into place to accommodate for the variability of 3DP. While ISO 10328 has been used in literature for the structural testing of prosthetic sockets, the standard is not designed for socket testing. In particular, ISO 10328 emphasizes distal end loading, while stresses such as the pressure distributions due to limb compliance are unaccounted for. To fully verify the safety of new socket designs, testing methods need to be further refined and implemented.<sup>17</sup>

This study presents only a proof of concept for producing engineered distal module geometry. Future research must continue to optimize and verify the design. To date, the design has only been tested by ultimate strength loading of one limb shape; future testing should incorporate a wide range of socket shapes and loading conditions to fully verify a final design. In particular, ISO 10328 cyclic loading should be emphasized to assess long term durability. Improvements to the design should minimize mass and reinforce weak areas. Decreasing build height will make the design viable for a wider

range of limb sizes and shapes, while a hollow or latticed interior could reduce mass while maintaining strength. Future designs should target the hex nut slots as a potential weak point, either better distributing stress across its geometry or replacing the feature with a stronger connection method.

Additional designs could also be created to enable a wider range of use cases. Models for additional suspension methods should be considered, as should adjustments for other 3DP methods. While Multi Jet Fusion is ideal for prosthetic sockets due to strong interlayer bonding mitigating failure along print layers, consideration should be placed into how design criteria may differ for additional printing methods. With 3DP often seen as desirable for low resource environments, adaptations for low end printing methods should be emphasized.

## **Conclusions**

Using topology optimization as a framework, a distal module was designed for use in transtibial sockets satisfying ISO 10328 ultimate strength standards at the P6 load level. FEA was performed to assess the role of build height and merging radius on the strength of sockets designed with the distal module. Three 3D-printed sockets were then tested using ISO 10328 ultimate strength standards to verify these FEA results. FEA results suggest socket strength has an inverse relationship to distal module build height and merging radius. A merging radius of 6 cm was recommended as the safety criteria for the current model, with build height recommended to be set as low as possible while still accommodating the given merging radius. Experimental testing demonstrated these criteria produced a socket capable of withstanding P6 loading while providing further evidence for the validity of FEA results. While these results provide a framework for producing a verified distal module, further research must be done to refine the design while verifying over a range of loading conditions and socket shapes. As the use of 3DP in prosthetics continues to grow, it is important to develop designs and techniques that fully utilize the unique strengths of this medium.

## Bibliography

1. Gariboldi F, Pasquarelli D, Cutti AG. Structural testing of lower-limb prosthetic sockets: a systematic review. *Med Eng Phys.* 2022;99. doi: 10.1016/j.medengphy.2021.103742
2. International Organization for Standardization. ISO 10328 Prosthetics—structural testing of lower limb prostheses—requirements and test methods. ISO 10328:2016 (E).
3. Pousett B, Lizcano A, Raschke SU. An investigation of the structural strength of transtibial sockets fabricated using conventional methods and rapid prototyping techniques. *Can Prosthet Orthot J.* 2019;2(1):31008. doi: 10.33137/cpoj.v2i1.31008
4. Gariboldi F, Scapinello M, Petrone N, Migliore GL, Teti G, Cutti AG. Static strength of lower-limb prosthetic sockets: an exploratory study on the influence of stratigraphy, distal adapter and lamination resin. *Med Eng Phys.* 2023;114:103970. doi: 10.1016/j.medengphy.2023.103970
5. Gerschutz MJ, Haynes ML, Nixon DM, Colvin JM. Strength evaluation of prosthetic check sockets, copolymer sockets, and definitive laminated sockets. *J Rehabil Res Dev.* 2012;49:405–426. doi: 10.1682/jrrd.2011.05.0091
6. Campbell AI, Sexton S, Schaschke CJ, et al. Prosthetic limb sockets from plant-based composite materials. *Prosthet Orthot Int* 2012;36:181–189. doi: 10.1177/0309364611434568

7. Graebner RH, Current TA. Relative strength of pylon-to-socket attachment systems used in transtibial composite sockets. *J Prosthet Orthot.* 2007;19(3):67-74. doi: 10.1097/jpo.0b013e3180cfe8da
8. Current TA, Kogler GF, Barth DG. Static structural testing of trans-tibial composite sockets. *Prosthet Orthot Int.* 1999;23(2):113-122. doi: 10.3109/03093649909071622
9. van der Stelt M, Verhamme L, Slump CH, Brouwers L, Maal TJ. Strength testing of low-cost 3D-printed transtibial prosthetic socket. *Proc Inst Mech Eng H.* 2022;236(3):367-375. doi: 10.1177/09544119211060092
10. Owen MK, DesJardins JD. Transtibial prosthetic socket strength: the use of ISO 10328 in the comparison of standard and 3D-printed sockets. *J Prosthet Orthot.* 2020;32(2):93-100. doi: 10.1097/jpo.0000000000000306
11. Faustini MC, Neptune RR, Crawford RH, Rogers WE, Bosker G. An experimental and theoretical framework for manufacturing prosthetic sockets for transtibial amputees. *IEEE Trans Neural Syst Rehabil Eng.* 2006;14(3):304-310. doi: 10.1109/TNSRE.2006.881570
12. Ribeiro D, Cimino SR, Mayo AL, Ratto M, Hitzig SL. 3D printing and amputation: a scoping review. *Disabil Rehabil Assist Technol.* 2021;16(2):221-240. doi: 10.1080/17483107.2019.1646825
13. Marinopoulos T, Li S, Silberschmidt VV. Mechanical performance of 3D printed prosthetic sockets: an experimental and numerical study. *Procedia Struct Integr.* 2022;42:903-910. doi: 10.1016/j.prostr.2022.12.114

14. Lindberg A, Alfthan J, Pettersson H, Flodberg G, Yang L. Mechanical performance of polymer powder bed fused objects – FEM simulation and verification. *Addit Manuf.* 2018;24:577-586. doi: 10.1016/j.addma.2018.10.009
15. Hewlett-Packard Company. HP 3D High Reusability CB PA 12. 4AA7-2469ENA:January 2019 (E).
16. International Organization for Standardization. ISO 527-2 Plastics—determination of tensile properties—part 2: test conditions for moulding and extrusion plastics. ISO 527-2:2012 (E).
17. Gariboldi F, Cutti AG, Fatone S, et al; AOPA Socket Guidance Workgroup. Mechanical testing of transtibial prosthetic sockets: A discussion paper from the American Orthotic and Prosthetic Association Socket Guidance Workgroup. *J Prosthet Orthot.* 2023;47(1):3-12. doi: 10.1097/jpo.0000000000000222